Anita Zeidler*, Philip Stephen Salmon, Andrea Piarristeguy, Annie Pradel, and Henry Edward Fischer

Structure of Glassy Ag–Ge–Se by Neutron Diffraction with Isotope Substitution

DOI 10.1515/zpch-2015-0727
Received November 2, 2015; accepted November 24, 2015

Abstract: The structure of glassy $Ag_{0.077}Ge_{0.212}Se_{0.711}$, which lies at $y = 0.077$ on the $Ag_y(Ge_{0.23}Se_{0.77})_{1-y}$ tie-line, was investigated by using the method of neutron diffraction with silver isotope substitution. Two glass transition temperatures were found from a characterisation of the material using modulated differential scanning calorimetry, which indicates a mixed phase material. The diffraction method provides site-specific information on the Ag coordination environment, and gives an average of 3.5(1) Ag–Se nearest-neighbours with a bond distance of 2.65(1) Å together with 0.9(1) Ag–Ag next nearest-neighbours at a distance of 2.9(2) Å. The incorporation of silver does not appear to have a marked effect on the coordination number of Se to other matrix (Ge or Se) atoms, which supports the notion that Ag forms dative bonds with Se lone-pair electrons. A model is given for predicting the change in the Se to matrix atom coordination number when a monovalent metal such as Ag is added to a Se rich Ge–Se base glass.

Keywords: Glass Structure, Neutron Diffraction, Isotope Substitution, Differential Scanning Calorimetry.

1 Introduction

The Ge_xSe_{1-x} system forms semiconducting glasses over a wide range of compositions ($0 \leq x \leq 0.43$) [1, 2], and is a model system for investigating the topological

***Corresponding author: Anita Zeidler,** Department of Physics, University of Bath, BA2 7AY Bath, United Kingdom, e-mail: a.zeidler@bath.ac.uk
Philip Stephen Salmon: Department of Physics, University of Bath, BA2 7AY Bath, United Kingdom
Andrea Piarristeguy, Annie Pradel: Institut Charles Gerhardt, UMR 5253 CNRS, CC 1503, Université de Montpellier, Pl. E. Bataillon, F-34095, Montpellier Cedex 5, France
Henry Edward Fischer: Institut Laue–Langevin, 71 Avenue des Martyrs CS 20156, F-38042, Grenoble Cedex 9, France

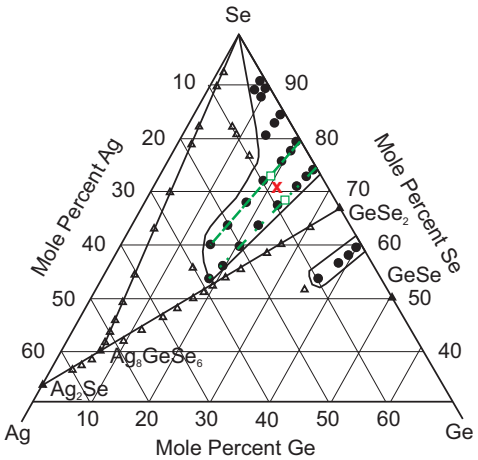

Figure 1: Glass formation in the Ag–Ge–Se system, as adapted from Borisova et al. [7], where glass forming compositions are identified by filled circles (●) and compositions showing partial crystallinity are identified by open triangles (△). The broken and chained (green) curves show the $Ag_y(Ge_{0.2}Se_{0.8})_{1-y}$ and $Ag_y(Ge_{0.25}Se_{0.75})_{1-y}$ tie-lines, respectively, and the (green) squares (□) on these tie-lines mark the compositions at which the glass becomes a fast-ion conductor with increasing Ag content [14]. Scanning electron microscope images show composition-dependent phase-separation on the scale of ≈ 160 nm–2 μm for the $x = 0.20$ tie-line and on the scale of ≈ 110 nm–0.7 μm for the $x = 0.25$ tie-line [14]. The (red) cross (×) identifies the composition studied in the present work.

ordering in disordered network-forming systems [3–6]. The network structure and its properties can be transformed by the addition of a network modifier, and there has been particular interest in the Ag–Ge–Se system where the addition of Ag can lead to the onset of fast-ion conductivity [7–13]. For instance, in the case of the $Ag_y(Ge_xSe_{1-x})_{1-y}$ ($0 \leq y \leq 1$) tie-lines with $x = 0.20$ and $x = 0.25$ (Figure 1), the ionic conductivity associated with Ag^+ ions increases dramatically at a composition $y \gtrsim 0.08$ [8–12]. Here, surface microscopy experiments show that the glass is phase separated into silver-rich and silver-poor phases, and the sharp increase in the ionic conductivity is believed to originate from a percolation of the silver-rich phase to form extended conduction pathways [11, 13–17]. The microscopic structure of these phases is, however, the subject of debate, and there have been several investigations using diffraction and/or modelling methods such as molecular dynamics and reverse Monte Carlo [18–30]. It is notable that thin films of amorphous Ag–Ge–Se can be used for making non-volatile programmable metallisation cell devices, where the application of an electric field induces the growth of conductive silver-rich 'nanowires' [27, 31–33]. In these devices, the solid-state electrolyte is made by the photo-diffusion of silver into a Se-rich Ge–Se base glass, where the

photoconductivity changes with variables such as the glass composition, light intensity, illumination time and temperature [34–36].

In this paper we investigate the structure of $Ag_{0.077}Ge_{0.212}Se_{0.711}$ glass by using the method of neutron diffraction with Ag isotope substitution, which was first applied to chalcogenide glasses by Penfold and Salmon [37]. This material lies on the $Ag_y(Ge_{0.23}Se_{0.77})_{1-y}$ tie-line at $y = 0.077$, i.e. around the percolation threshold for the ionic conductivity [14]. Its characterisation using modulated differential scanning calorimetry (MDSC) indicates two glass transition temperatures. The diffraction method enables the μ–μ' pair-correlation functions to be eliminated from a measured diffraction pattern, where μ (or μ') denotes a matrix atom (Ge or Se), and thus provides site-specific information on the Ag coordination environment. Additionally, the Ag-μ pair-correlation functions can be eliminated, which also simplifies the complexity of correlations associated with a single diffraction pattern [38]. We find an average of 3.5(1) Ag–Se nearest neighbours with a bond distance of 2.65(1) Å, and an average of 0.9(1) Ag–Ag next nearest-neighbours at a distance of 2.9(2) Å, as averaged over the different phases present. The results also suggest a local μ–μ' coordination environment that is similar to that of glassy $Ge_{0.23}Se_{0.77}$ [39].

The manuscript is organised as follows. In Section 2 the essential theory is described for the method of neutron diffraction with Ag isotope substitution. The experimental details are described in Section 3 and the results are presented in Section 4. The results are discussed in Section 5 and conclusions are drawn in Section 6.

2 Neutron diffraction theory

In a neutron diffraction experiment the total structure factor [40]

$$F(q) = \sum_{\alpha}\sum_{\beta} c_\alpha c_\beta b_\alpha b_\beta [S_{\alpha\beta}(q) - 1] \tag{1}$$

is measured where q denotes the magnitude of the scattering vector, c_α and b_α are the atomic fraction and coherent neutron scattering length of chemical species α, respectively, and $S_{\alpha\beta}(q)$ is a so-called Faber–Ziman [41] partial structure factor. The latter is related to the partial pair-distribution function $g_{\alpha\beta}(r)$ via the Fourier transform relation

$$g_{\alpha\beta}(r) - 1 = \frac{1}{2\pi^2 \rho r}\int_0^\infty \mathrm{d}q\, q\, [S_{\alpha\beta}(q) - 1]\sin(qr) \tag{2}$$

where ρ is the atomic number density and r is a distance in real space. These $g_{\alpha\beta}(r)$ functions give a measure of the probability of finding two atoms of type α and β separated by a distance r, and are defined such that the mean coordination number of atoms of type β in a spherical shell defined by radii r_i and r_j around a central atom of type α is given by

$$\bar{n}_{\alpha}^{\beta} = 4\pi\rho\, c_{\beta} \int_{r_i}^{r_j} \mathrm{d}r\, r^2\, g_{\alpha\beta}(r). \tag{3}$$

Let neutron diffraction experiments be performed on two Ag–Ge–Se glasses that are identical in every respect, except that one of the materials contains ^{107}Ag and the other contains ^{109}Ag. If the measured total structure factors are denoted by $^{107}F(q)$ and $^{109}F(q)$, respectively, then the difference function

$$\begin{aligned} \Delta F_{\mathrm{Ag}}(q) &\equiv {}^{107}F(q) - {}^{109}F(q) \\ &= 2c_{\mathrm{Ag}}\Delta b_{\mathrm{Ag}} \left\{ \sum_{\alpha\neq\mathrm{Ag}} c_{\alpha} b_{\alpha} [S_{\mathrm{Ag}\alpha}(q) - 1] \right\} \\ &\quad + c_{\mathrm{Ag}}^2 \left(b_{^{107}\mathrm{Ag}}^2 - b_{^{109}\mathrm{Ag}}^2 \right) [S_{\mathrm{AgAg}}(q) - 1] \end{aligned} \tag{4}$$

eliminates all of the correlations that do not involve Ag, where $\Delta b_{\mathrm{Ag}} = b_{^{107}\mathrm{Ag}} - b_{^{109}\mathrm{Ag}}$.

It is also possible to eliminate the Ag-μ pair-correlations from a total structure factor, where μ denotes a matrix atom (Ge or Se), via the difference function

$$\begin{aligned} \Delta F(q) &\equiv \left[b_{^{107}\mathrm{Ag}}\, {}^{109}F(q) - b_{^{109}\mathrm{Ag}}\, {}^{107}F(q) \right] / \Delta b_{\mathrm{Ag}} \\ &= \Delta F_{\mu\mu'}(q) - c_{\mathrm{Ag}}^2 b_{^{107}\mathrm{Ag}} b_{^{109}\mathrm{Ag}} [S_{\mathrm{AgAg}}(q) - 1] \end{aligned} \tag{5}$$

where $\Delta F_{\mu\mu'}(q) = \sum_{\alpha\neq\mathrm{Ag}} \sum_{\beta\neq\mathrm{Ag}} c_{\alpha} c_{\beta} b_{\alpha} b_{\beta} [S_{\alpha\beta}(q) - 1]$ contains information only on those pair-correlation functions describing the matrix atoms.

The real-space functions corresponding to $F(q)$, $\Delta F_{\mathrm{Ag}}(q)$ and $\Delta F(q)$ are denoted by $G(r)$, $\Delta G_{\mathrm{Ag}}(r)$ and $\Delta G(r)$, respectively, and are obtained by Fourier transformation. For example, the total pair-distribution function $G(r)$ is given by

$$G(r) = \frac{1}{2\pi^2 \rho\, r} \int_0^{\infty} \mathrm{d}q\, q\, F(q) M(q) \sin(qr) \tag{6}$$

where $M(q)$ is a modification function defined by $M(q) = 1$ for $q \leq q_{\max}$, $M(q) = 0$ for $q > q_{\max}$. The latter is introduced because a diffractometer can measure only over a finite scattering vector range up to a maximum value $q_{\max}$. This modification function can lead to Fourier transform artifacts that can be particularly

notable for the first real-space peak. However, if q_{max} is sufficiently large that the q-space functions no longer show structure, then q_{max} will not introduce Fourier transform artifacts such that $G(r)$, $\Delta G_{Ag}(r)$ and $\Delta G(r)$ are given by Equations (1), (4) and (5), respectively, after each $S_{\alpha\beta}(q)$ function is replaced by the corresponding $g_{\alpha\beta}(r)$ function. Thus, $\Delta G_{Ag}(r)$ will provide site-specific structural information on the Ag coordination environment where, in the present experiment, the weighting factors for the Ag–Ge, Ag–Se and Ag–Ag partial pair-correlation functions are 9.005(47), 29.4(1) and 2.35(1) mbarn, respectively. In comparison, $\Delta G(r)$ will be dominated by the μ–μ' partial pair-correlation functions where, in the present experiment, the weighting factors for the Ge–Ge, Ge–Se, Se–Se and Ag–Ag partial pair-correlation functions are 30(1), 196.6(5), 320.7(7) and −1.89(6) mbarn, respectively.

3 Experimental details

3.1 Sample preparation

Glassy samples of $Ag_{0.077}Ge_{0.212}Se_{0.711}$ were prepared by mixing $Ag_{0.25}(Ge_{0.25}Se_{0.75})_{0.75}$ glass powder, containing either ^{107}Ag (99.50% enrichment, Isoflex) or ^{109}Ag (99.40% enrichment, Isoflex), with the requisite amount of Ge (99.999%, Sigma Aldrich) and Se (≥ 99.999%, Sigma Aldrich) powder. These powders were loaded into silica ampoules of 5 mm inner diameter and 1 mm wall thickness within a high-purity Ar filled glovebox. (The ampoules had first been cleaned with 48 wt. % hydrofluoric acid, rinsed with water then acetone, dried, and baked-out under vacuum at a temperature of 800 °C for 3 h.) Each of the sample containing ampoules was then evacuated, sealed under a pressure of ≈ 10^{-5} Torr, and placed into a rocking furnace where the temperature was increased to 962 °C (the melting point of Ag) at a ramp rate of 1 °C/min, dwelling for 4 h each at 221 °C (the melting point of Se), 685 °C (the boiling point of Se) and 938 °C (the melting point of Ge). At 962 °C the temperature was kept constant for 18 h, after which the rocking motion was stopped, the furnace was placed vertically to allow the liquid sample to collect at the bottom of the ampoule, and after a further 6 h the temperature was decreased to 800 °C at a ramp rate of 1 °C/min where it was kept for an additional 5 h. Finally, the sample was quenched by dropping the ampoule into an ice/water mixture. Each ampoule was broken open inside a high-purity Ar filled glovebox, where the sample was loaded into the vanadium container used for the diffraction experiment.

3.2 Neutron diffraction & MDSC

The diffraction experiment was performed at room temperature ($\simeq 25\,^{\circ}$C) using the D4c instrument at the Institut Laue–Langevin in Grenoble, France [42] with an incident neutron wavelength of 0.4961(1) Å. Diffraction patterns were measured for the samples in a cylindrical vanadium container of inner diameter 6.80(1) mm and wall thickness 0.10(1) mm, the empty container, a cylindrical vanadium rod of 6.37(1) mm diameter for normalisation purposes, the empty instrument, and an absorbing bar of $^{10}B_4C$ having dimensions comparable to the sample to account for the effect of the sample self-attenuation on the background signal at small scattering angles. To test the stability of the instrument, the measured intensity for a given setup was saved at regular intervals, and the ratio between these intensities showed no deviation within the statistical error. The data correction procedure is described in detail elsewhere [43]. The neutron scattering lengths are $b_{Ge} = 8.185(20)$, $b_{Se} = 7.970(9)$, $b_{^{107}Ag} = 7.538(11)$ and $b_{^{109}Ag} = 4.185(11)$ fm, which take into account the isotopic enrichment of the silver isotopes [44]. The number density of the glass was measured to be $\rho = 0.0374(1)$ Å^{-3} using a Quantachrome MICRO-ULTRAPYC 1200*e* pycnometer.

The glass transition temperature T_g was measured using a TA Instruments Q100 modulated differential scanning calorimeter with a scan rate of 3 $^{\circ}$C/min, modulation of $\pm 1\,^{\circ}$C per 100 s, and an oxygen-free nitrogen gas flow rate of 25 ml/min. Scans were made by increasing the temperature from 150 $^{\circ}$C to 260 $^{\circ}$C, and the T_g values were taken from the onset of changes to the total heat capacity. The MDSC experiments showed two T_g values of 187 (2) $^{\circ}$C and 222 (1) $^{\circ}$C, which indicates a phase separated glass (Section 5). These glass transition temperatures compare to a value of $T_g = 197$ (1) $^{\circ}$C as measured using the same method for glassy $Ge_{0.23}Se_{0.77}$ [39], i.e. for the matrix material in which the Ag is dissolved.

4 Results

The measured total structure factors $F(q)$ (Figure 2) are characterised by a first sharp diffraction peak at 1.07(1) Å^{-1}, a principal peak at 2.02(1) Å^{-1} and a third peak at 3.51(1) Å^{-1}. The corresponding total pair-distribution functions $G(r)$ (Figure 3) have a first peak at 2.36(1) Å that arises from an overlap of μ–μ' correlations [45], and a next higher-r feature that corresponds to Ag–Se nearest-neighbours (see below). To account for the effect of the finite q_{max} value of the diffractometer (Section 2), the first peak in the function $D(r) \equiv 4\pi\rho r G(r)/|G(r \to 0)|$ was fitted to a sum of two Gaussian functions, each convoluted with

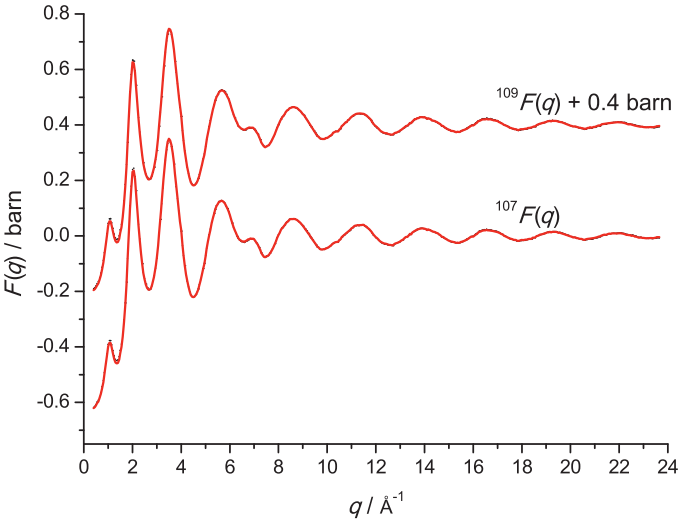

Figure 2: The measured total structure factors $F(q)$ for $Ag_{0.077}Ge_{0.212}Se_{0.711}$ glass. The points with vertical (black) error bars show the measured data sets, and the solid (red) curves show the back-Fourier transforms of the corresponding $G(r)$ functions given by the solid curves in Figure 3. The error bars are smaller than the line thickness at most q values.

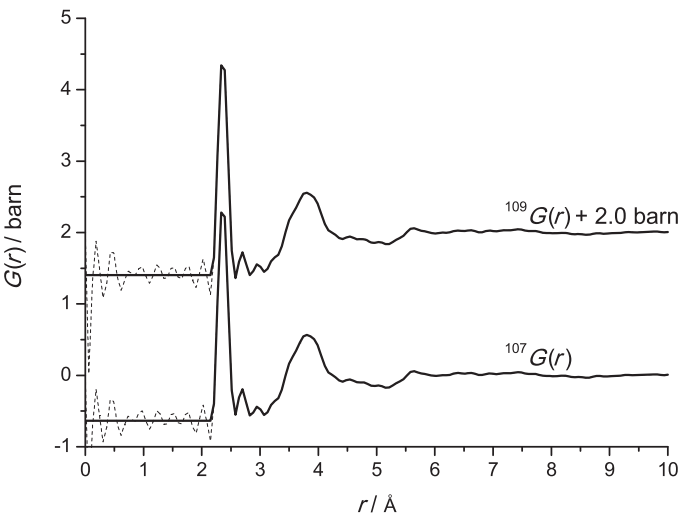

Figure 3: The measured total pair-distribution functions $G(r)$ for $Ag_{0.077}Ge_{0.212}Se_{0.711}$ glass. The solid curves show the Fourier transforms of the measured data sets given in Figure 2 after the unphysical oscillations at r-values smaller than the distance of closest approach between two atoms are set to the theoretical $G(r \to 0)$ limit. The broken curves show the extent of these oscillations.

the Fourier transform of the modification function $M(q)$ [46]. In this analysis it was assumed that there are contributions solely from Ge–Se and Se–Se correlations with $\bar{n}_{\mathrm{Ge}}^{\mathrm{Se}} = 4$. This assignment is consistent with a chemically ordered network model for the Se-rich Ge–Se base glass (see Section 5), and the presence of $GeSe_4$ motifs in the modified glass is supported by inelastic neutron scattering and Raman spectroscopy experiments on glassy $Ag_{0.25}(Ge_{0.25}Se_{0.75})_{0.75}$ [47]. The fits give a Ge–Se distance of 2.365(5) Å, a Se–Se distance of 2.355(5) Å and a coordination number $\bar{n}_{\mathrm{Se}}^{\mathrm{Se}} = 0.81(4)$. A similar analysis of the neutron diffraction results for glassy $Ag_{0.1}(Ge_{0.25}Se_{0.75})_{0.9}$ with $\bar{n}_{\mathrm{Ge}}^{\mathrm{Se}} = 4$ gives $\bar{n}_{\mathrm{Se}}^{\mathrm{Se}} = 0.90$ [26].

The measured difference function $\Delta F_{\mathrm{Ag}}(q)$ (Figure 4(a)) shows an increase of intensity at small q-values that is likely to originate from the glass inhomogeneity indicated by the MDSC results. A similar feature has been observed for the $\Delta F_{\mathrm{Ag}}(q)$ functions measured for glasses in the Ag–As–Se system [48]. The corresponding r-space function $\Delta G_{\mathrm{Ag}}(r)$ (Figure 5(a)) has a first peak at 2.67(1) Å with a shoulder at ≃ 3 Å, where the effect of the finite q_{max} value of the diffractometer can be neglected. In comparison, the crystalline polymorphs of Ag_8GeSe_6 have structures in which Ge is 4-fold coordinated to Se atoms, Ag is bound to 3 or 4 Se atoms, and the shortest Ag–Ag distance is ≃ 3 Å. In the β'-Ag_8GeSe_6 phase, for example, Ag is bonded to 3 or 4 Se atoms at distances in the range 2.53–2.91 Å and the shortest Ag–Ag distances are in the range 2.99–3.18 Å [49].

The first peak in $\Delta G_{\mathrm{Ag}}(r)$ was therefore fitted to a sum of three Gaussian functions, where the first was attributed to Ag–Se correlations, the second to Ag–Ag correlations, and the third to a mixture of both Ag–Se and Ag–Ag correlations (Figure 5(a)). The results give a Ag–Se bond distance of 2.65(1) Å with $\bar{n}_{\mathrm{Ag}}^{\mathrm{Se}} = 3.5(1)$ and a nearest-neighbour Ag–Ag distance of 2.9(2) Å with $\bar{n}_{\mathrm{Ag}}^{\mathrm{Ag}} = 0.9(1)$. In comparison, for the glassy fast-ion conductor $Ag_{0.25}(Ge_{0.25}Se_{0.75})_{0.75}$, anomalous X-ray scattering experiments give a Ag–Se bond distance of 2.62 Å with a Ag–Se coordination number in the range 3.9–4.6 and a nearest-neighbour Ag–Ag distance ≃ 3.35 Å [19], whereas neutron diffraction experiments give a Ag–Se bond distance of 2.68(1) Å with $\bar{n}_{\mathrm{Ag}}^{\mathrm{Se}} = 3.0(1)$ and a nearest-neighbour Ag–Ag distance of 3.02(5) Å with $\bar{n}_{\mathrm{Ag}}^{\mathrm{Ag}} = 4.2(2)$ [22]. For glassy $Ag_{0.1}(Ge_{0.4}Se_{0.6})_{0.9}$, which is not expected to be a fast-ion conductor [7], anomalous X-ray scattering experiments give a Ag–Se bond distance of 2.65(2) Å with $\bar{n}_{\mathrm{Ag}}^{\mathrm{Se}} = 3.9(3)$ [18]. For liquid Ag_2Se, the measured $g_{\mathrm{AgSe}}(r)$ function has a first peak at 2.60(5) Å and the measured $g_{\mathrm{AgAg}}(r)$ function has a first peak at 2.80(5) Å with only a weak minimum on its high-r side [50].

The measured difference function $\Delta F(q)$ (Figure 4(b)) is dominated by the μ–μ' correlations, and the first three peaks appear at 1.10(1), 2.02(1) and 3.54(1) $\mathrm{Å}^{-1}$. This three-peak profile is typical of binary Ge–Se glasses [45].

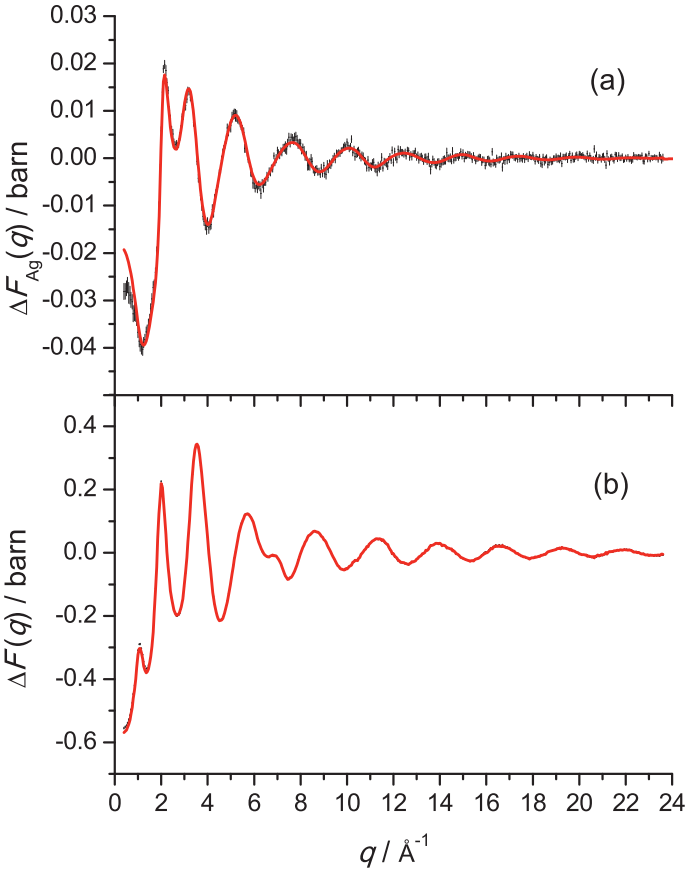

Figure 4: The measured difference functions (a) $\Delta F_{Ag}(q)$ and (b) $\Delta F(q)$ for $Ag_{0.077}Ge_{0.212}Se_{0.711}$ glass. The points with vertical (black) error bars show the measured data sets, and the solid (red) curves show the back-Fourier transforms of the corresponding $\Delta G_{Ag}(r)$ and $\Delta G(r)$ functions given by the solid curves in Figure 5. In (b) the error bars are smaller than the line thickness at most q values.

The first peak at 2.36(1) Å in the corresponding r-space function $\Delta G(r)$ (Figure 5(b)) arises from μ–μ' correlations. To account for the effect of the finite q_{max} value of the diffractometer (Section 2), the corresponding feature in $\Delta D(r) \equiv 4\pi\rho r\Delta G(r)/|\Delta G(r \to 0)|$ was fitted to a sum of two Gaussian functions, each convoluted with the Fourier transform of the modification function $M(q)$ [46]. Here, the analysis followed the prescription used for the $D(r)$ functions, i.e. it was assumed that the first peak comprises solely Ge–Se and Se–Se correlations with a coordination number $\bar{n}_{Ge}^{Se} = 4$. Hence, a Ge–Se distance of 2.365(5) Å is

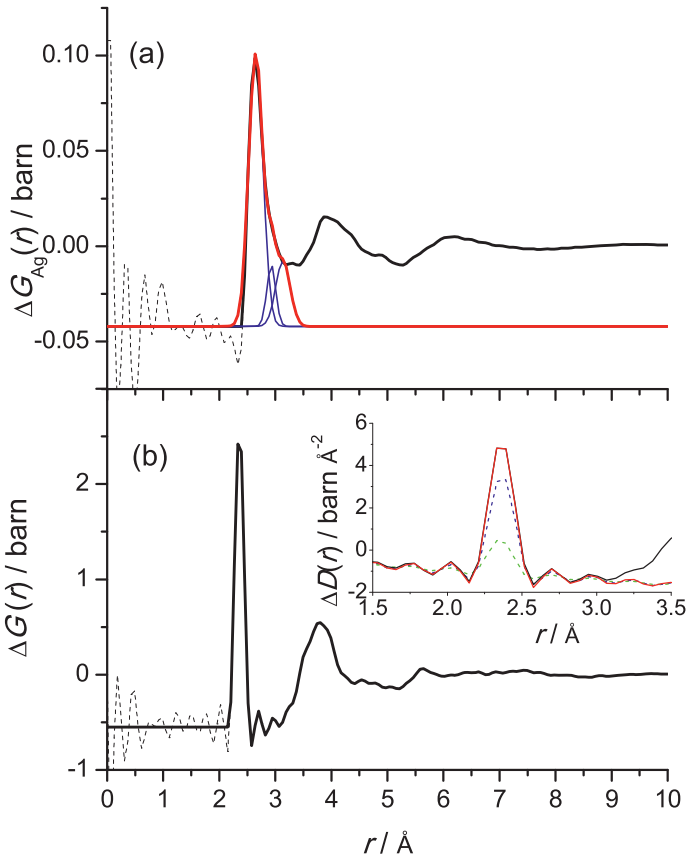

Figure 5: The measured difference functions (a) $\Delta G_{Ag}(r)$ and (b) $\Delta G(r)$ for $Ag_{0.077}Ge_{0.212}Se_{0.711}$ glass. The solid (black) curves show the Fourier transforms of the data sets given in Figure 4 after the unphysical oscillations at r-values smaller than the distance of closest approach between two atoms are set to the theoretical (a) $\Delta G_{Ag}(r \to 0)$ or (b) $\Delta G(r \to 0)$ limit. The broken curves show the extent of these oscillations. In (a) the thin solid (blue) curves give the Gaussian functions that were fitted to the data, and the solid (red) curve is the sum of these Gaussians. In (b) the inset shows the fit (solid light (red) curve) of the first peak in $\Delta D(r)$ (solid dark (black) curve) to a sum of two Gaussian functions representing the Ge–Se (broken dark (blue) curve) and Se–Se (broken light (green) curve) correlations, each convoluted with the Fourier transform of the modification function $M(q)$.

obtained, along with a Se–Se distance of 2.355(5) Å and a coordination number $\bar{n}_{Se}^{Se} = 0.81(4)$.

5 Discussion

Wang et al. [51] used MDSC to investigate glasses along the $Ag_y(Ge_xSe_{1-x})_{1-y}$ tie-lines with $x = 0.20$ and 0.25 (Figure 1). For each of these tie-lines, two glass transition temperatures $T_g(1)$ and $T_g(2)$ were found, where the values were taken from the inflection point of the reversing heat flow. For the $x = 0.20$ tie-line, $T_g(1) \approx 180\,^{\circ}C$ at $y = 0.02$ and increased with the Ag content of the glass to give $T_g(1) \approx 200\,^{\circ}C$ at $y = 0.20$, while $T_g(2) \approx 230\,^{\circ}C$ and did not change with the Ag content (see also [52]). For the $x = 0.25$ tie-line, $T_g(1) \approx 230\,^{\circ}C$ and increased with the Ag content of the glass, while a second transition at $T_g(2) \approx 230\,^{\circ}C$ could be observed at $y = 0.10$ and did not change markedly with the Ag content. The emergence of two T_g values was interpreted in terms of phase separation into a silver-free Ge–Se 'base glass' and an Ag_2Se-rich 'additive glass' [51, 52]. As the Ag-content increases along a given tie-line, the composition of the additive glass was deemed to be invariant such that its T_g value does not vary with y, a scenario that necessitates a change in composition of the base glass such that its T_g value increases with y. In comparison, phase separation into silver-rich and silver-poor glassy phases has been observed for the $Ag_y(Ge_xSe_{1-x})_{1-y}$ tie-lines ($x = 0.20$, 0.25) from scanning electron microscopy (SEM) [11, 13, 14], electric force microscopy (EFM) [15–17] and conductive atomic force microscopy (C-AFM) [16] experiments, but the EFM and C-AFM results indicate a composition for the Ag rich phase that is not constant along a given tie-line. We note that two T_g values were also found in MDSC work on samples of composition $Ge_{0.15}Se_{0.85-y}Ag_y$ with $0 \le y \le 0.20$ [53]. Multiple glass transitions were not, however, seen in DSC work on $Ag_y(Ge_{0.25}Se_{0.75})_{1-y}$ glasses [8, 11, 54] or in DSC work on glassy $Ag_{0.33}(Ge_{0.2537}Se_{0.7463})_{0.67}$ (i.e. $Ag_{33}Ge_{17}Se_{50}$) [55].

In the present work, the glass composition can be written as $Ag_{0.077}(Ge_{0.23}Se_{0.77})_{0.923}$, i.e. $Ge_{0.23}Se_{0.77}$ can be considered to be a base glass to which Ag is added. It is therefore of interest to consider the structure of the pure base-glass, which has been investigated by neutron diffraction [39], in order to determine the effect of Ag on its structure. If the first peak in the measured $G(r)$ function for glassy $Ge_{0.23}Se_{0.77}$ is interpreted in the same way as for the Ag–Ge–Se glass (see Section 4), i.e. if it is assumed that it has contributions solely from Ge–Se and Se–Se correlations with a coordination number $\bar{n}_{Ge}^{Se} = 4$, then a Se–Se coordination number $\bar{n}_{Se}^{Se} = 0.81(4)$ is obtained, which is in accord with the value $\bar{n}_{Se}^{Se} = 0.805$ expected for a chemically ordered continuous random network model [45]. For glassy $Ge_{0.23}Se_{0.77}$, it is also possible to exploit the similarity between the coherent neutron scattering lengths of Ge and Se of natural isotopic abundance to calculate the Bhatia-Thornton [56] number-number partial

pair-distribution function

$$g_{\mathrm{NN}}(r) \equiv c_{\mathrm{Ge}}^2 g_{\mathrm{GeGe}}(r) + 2c_{\mathrm{Ge}}c_{\mathrm{Se}}g_{\mathrm{GeSe}}(r) + c_{\mathrm{Se}}^2 g_{\mathrm{SeSe}}(r) \simeq [G(r) - G(r \to 0)]/\langle b \rangle^2 \quad (7)$$

where the mean coherent scattering length $\langle b \rangle = (c_{\mathrm{Ge}}b_{\mathrm{Ge}} + c_{\mathrm{Se}}b_{\mathrm{Se}})/(c_{\mathrm{Ge}} + c_{\mathrm{Se}})$ and $G(0) = -\langle b \rangle^2$. This function describes the topological ordering in the glass [57], and its integration gives an overall mean coordination number $\bar{n} = 4\pi\rho \int_{r_i}^{r_j} \mathrm{d}r\, r^2\, g_{\mathrm{NN}}(r)$ which does not depend on any assumption about the chemical ordering [45]. This coordination number can be expressed as (Appendix A)

$$\bar{n} = \frac{c_{\mathrm{Ge}}}{c_{\mathrm{Ge}} + c_{\mathrm{Se}}}\bar{n}_{\mathrm{Ge}} + \frac{c_{\mathrm{Se}}}{c_{\mathrm{Ge}} + c_{\mathrm{Se}}}\bar{n}_{\mathrm{Se}}, \quad (8)$$

where the mean Ge coordination number $\bar{n}_{\mathrm{Ge}} = \bar{n}_{\mathrm{Ge}}^{\mathrm{Ge}} + \bar{n}_{\mathrm{Ge}}^{\mathrm{Se}}$, the mean Se coordination number $\bar{n}_{\mathrm{Se}} = \bar{n}_{\mathrm{Se}}^{\mathrm{Se}} + \bar{n}_{\mathrm{Se}}^{\mathrm{Ge}}$, and it follows from Equation (3) that $\bar{n}_{\mathrm{Se}}^{\mathrm{Ge}} = (c_{\mathrm{Ge}}/c_{\mathrm{Se}})\bar{n}_{\mathrm{Ge}}^{\mathrm{Se}}$. The neutron diffraction results for glassy $Ge_{0.23}Se_{0.77}$ [39] give $\bar{n} = 2.46(1)$, in full accord with the value $\bar{n} = 2.46$ expected on the basis of the '8-N' rule for which $\bar{n}_{\mathrm{Ge}} = 4$ and $\bar{n}_{\mathrm{Se}} = 2$. The values of $\bar{n}_{\mathrm{Ge}}^{\mathrm{Se}} = 4$ and $\bar{n}_{\mathrm{Se}}^{\mathrm{Se}} = 0.81(4)$ found by assuming a chemically ordered network are also consistent with the '8-N' rule, and their substitution into Equation (8) gives $\bar{n} = 2.46(3)$.

For $Ag_{0.077}(Ge_{0.23}Se_{0.77})_{0.923}$ glass, the first peaks in $G(r)$ and $\Delta G(r)$ both yield coordination numbers of $\bar{n}_{\mathrm{Se}}^{\mathrm{Se}} = 0.81(4)$ with $\bar{n}_{\mathrm{Ge}}^{\mathrm{Se}} = 4$ that are in agreement with the results found for the base glass. These values, when substituted into Equation (8), also give $\bar{n} = 2.46(3)$, which is consistent with the '8-N' rule. A scenario where Ge and Se atoms remain 4-fold and 2-fold coordinated to other matrix atoms, respectively, is not, however, expected: The measured $\Delta G_{\mathrm{Ag}}(r)$ function (Figure 5(a)) shows the presence of Ag–Se nearest-neighbours, i.e. Ag is expected to displace Ge or Se as the nearest-neighbour atoms to Se. This substitution will reduce from two the number of matrix atoms surrounding Se and will hence lead to an $\bar{n}$ value that is lower than expected on the basis of the '8-N' rule. An explanation may lie with a propensity for Ag to form dative bonds with Se lone-pair electrons, as in Kastner's model where Ag will form one covalent bond with Se and up to three dative bonds to Se where each Se atom donates both of its lone-pair electrons to that bond [18, 22, 58]. In this case, the addition of a small amount of Ag to a base Ge–Se glass will result in a relatively small change to the Se-μ coordination number, thus making changes to $\bar{n}$ small and difficult to observe. As shown in Appendix B, if the addition of Ag breaks preferentially the Se–Se homopolar bonds of a Se-rich Ge–Se base glass then, for the case of glassy $Ag_{0.077}(Ge_{0.23}Se_{0.77})_{0.923}$, the mean Se-$\mu$ coordination number will reduce from $\bar{n}_{\mathrm{Se}} = 2$ to $\bar{n}_{\mathrm{Se}} = 1.892$ such that there will be a $\simeq 3\%$ reduction in the mean μ–μ' coordination number from $\bar{n} = 2.46$ to $\bar{n} = 2.377$.

6 Conclusions

The structure and thermal properties of the chalcogenide glass $Ag_{0.077}Ge_{0.212}Se_{0.711}$ were measured by using neutron diffraction with silver isotope substitution and MDSC, respectively. Two glass transition temperatures were found along with an increase in intensity of $\Delta F_{Ag}(q)$ at low q-values, observations that support a phase separation of the material into silver-rich and silver-poor phases as reported for similar Ag–Ge–Se glasses from surface microscopy experiments. The addition of silver to the $Ge_{0.23}Se_{0.77}$ base glass does not appear to alter significantly the local structure of this glass at the pair-correlation function level. This observation suggests that Ag interacts predominantly with the Se lone-pair electrons.

Acknowledgement: We would like to thank Ozgur Gulbiten (Corning Inc.) and Phil Davies (TA Instruments) for helpful discussions on the interpretation of MDSC data. We would also like to thank the EPSRC for support to the Bath group via grant Nos. EP/G008795/1 and EP/J009741/1. AZ is supported by a Royal Society – EPSRC Dorothy Hodgkin Research Fellowship.

Appendix A

Equation (8) corresponds to the overall mean coordination number of just the matrix atoms in a ternary system such as Ag–Ge–Se, i.e.

$$\begin{aligned}\bar{n} &= \frac{N_{Ge}}{N_{Ge}+N_{Se}}\bar{n}_{Ge} + \frac{N_{Se}}{N_{Ge}+N_{Se}}\bar{n}_{Se} \\ &= \frac{c_{Ge}}{c_{Ge}+c_{Se}}\bar{n}_{Ge} + \frac{c_{Se}}{c_{Ge}+c_{Se}}\bar{n}_{Se}\end{aligned} \tag{9}$$

where N_α (α = Ge or Se) is the total number of α-type atoms in the material. For a two component Ge–Se system, $c_{Ge}+c_{Se} = 1$ and Equation (9) reduces to the usual expression [45]

$$\bar{n} = c_{Ge}\bar{n}_{Ge} + c_{Se}\bar{n}_{Se}. \tag{10}$$

For a ternary system such as $Ag_y(Ge_xSe_{1-x})_{1-y}$ it follows that $c_{Ge} + c_{Se} \neq 1$. Nevertheless, $c_{Ge}/(c_{Ge} + c_{Se}) = x$ and $c_{Se}/(c_{Ge} + c_{Se}) = 1 - x$ such that Equation (9) will give the expected value of $\bar{n}$ in the limit of complete phase separation of the material into Ag and base Ge–Se glass.

Appendix B

Consider a chemically ordered network model for a Ge_xSe_{1-x} glass ($0 \le x \le 1$) containing N_{Ge} Ge atoms and N_{Se} Se atoms in which the bonding follows the '8-N' rule, i.e. the coordination number of Ge $Z_{Ge} = 4$ and the coordination number of Se $Z_{Se} = 2$. Let the glass have a Se-rich composition $0 \le x < 1/3$ such that $\bar{n}_{Ge}^{Ge} = 0$. In the limit when $x = 0$, Se atoms will be bound solely to other Se atoms and the number of Se–Se bonds is given by $\mathcal{N}_{SeSe} = N_{Se}Z_{Se}/2$, where the factor of two avoids double counting. If x is then increased, $N_{Ge}Z_{Ge}/2$ Se–Se bonds will be broken by the formation of $N_{Ge}Z_{Ge}$ Ge–Se bonds, thus reducing the number of Se–Se bonds to $\mathcal{N}_{SeSe} = N_{Se}Z_{Se}/2 - N_{Ge}Z_{Ge}/2$. Then the mean Ge coordination number $\bar{n}_{Ge} = \bar{n}_{Ge}^{Se} = Z_{Ge}$, the coordination number of Ge around Se $\bar{n}_{Se}^{Ge} = x\bar{n}_{Ge}^{Se}/(1-x)$ from the definition given by Equation (3), and the Se–Se coordination number $\bar{n}_{Se}^{Se} = 2\mathcal{N}_{SeSe}/N_{Se}$. Hence, the mean Se coordination number $\bar{n}_{Se} = \bar{n}_{Se}^{Se} + \bar{n}_{Se}^{Ge} = Z_{Se}$, and Equation (8) can be re-written as $\bar{n} = xZ_{Ge} + (1-x)Z_{Se}$.

Let monovalent metal M atoms be added to this Se-rich Ge–Se base glass. The model of Kastner [58] predicts that each M atom will be four-fold coordinated by Se atoms when the covalent contribution to the bonding is significant and electronic d states are not involved. One of these M–Se bonds is formed by using the valence electron from M and a valence electron from Se, and the other three M–Se bonds are dative, using the lone pair electrons on three other Se atoms. This bonding scheme results in a single two-fold coordinated Se atom and three three-fold coordinated Se atoms, respectively. Let's assume that the M atoms break preferentially the homopolar Se–Se bonds. Then the addition of two M atoms will break a Se–Se bond to give two M–Se bonds, so the addition of N_M M atoms will lead to a reduction in the number of Se–Se bonds to $\mathcal{N}_{SeSe} = N_{Se}Z_{Se}/2 - N_{Ge}Z_{Ge}/2 - N_M/2$, resulting in a revised Se–Se coordination number $\bar{n}_{Se}^{Se} = 2\mathcal{N}_{SeSe}/N_{Se} = Z_{Se} - N_{Ge}Z_{Ge}/N_{Se} - N_M/N_{Se}$.

If the composition of the modified glass is written as $M_y(Ge_xSe_{1-x})_{1-y}$ where $0 \le x \le 1$ and $0 \le y \le 1$, then the ratio of $N_M : N_{Ge} : N_{Se}$ is given by $y : x(1-y) : (1-x)(1-y)$ and $\bar{n}_{Se}^{Ge} = x\bar{n}_{Ge}^{Se}/(1-x)$. It follows that the mean Se-μ coordination number for the modified glass can be expressed as $\bar{n}_{Se} = Z_{Se} - (N_M/N_{Se}) = Z_{Se} - [y/(1-x)(1-y)]$ such that Equation (8) can be re-written as

$$\bar{n} = xZ_{Ge} + (1-x)\left[Z_{Se} - \frac{y}{(1-x)(1-y)}\right], \tag{11}$$

where $Z_{Ge} = 4$ and $Z_{Se} = 2$. Hence, in the case of glassy $Ag_{0.077}(Ge_{0.23}Se_{0.77})_{0.923}$, the mean Se-$\mu$ coordination number $\bar{n}_{Se} = 1.892$ and the mean μ–μ' coordination number $\bar{n} = 2.377$. The latter compares to an '8-N' rule value of $\bar{n} = 2.46$, i.e. the

formation of dative bonds according to the model of Kastner [58] leads to only a $\simeq 3\%$ reduction in $\bar{n}$.

We note that d states may play an important role in the bonding in Ag(I) glasses. For example, an investigation of the relative stability of three-fold versus four-fold coordination complexes using a molecular orbital approach suggests that the lower-coordination-number conformation can be stabilized over the regular tetrahedral arrangement if there is a distortion via a second-order Jahn–Teller effect wherein the d orbitals of the occupied outer shell are mixed with the s orbitals of the valence shell [59].

References

1. R. Azoulay, H. Thibierge, and A. Brenac, J. Non-Cryst. Solids **18** (1975) 33.
2. Z. U. Borisova, *Glassy Semiconductors*, Plenum Press, New York (1981).
3. J. C. Phillips, J. Non-Cryst. Solids **34** (1979) 153.
4. M. F. Thorpe, J. Non-Cryst. Solids **57** (1983) 355.
5. A. Sartbaeva, S. A. Wells, A. Huerta, and M. F. Thorpe, Phys. Rev. B **75** (2007) 224204.
6. P. K. Gupta and J. C. Mauro, J. Chem. Phys. **130** (2009) 094503.
7. Z. U. Borisova, T. S. Rykova, E. Yu. Turkina, and A. R. Tabolin, Inorg. Mater. **20** (1985) 1558.
8. M. Kawasaki, J. Kawamura, Y. Nakamura, and M. Aniya, Solid State Ionics **123** (1999) 259.
9. M. Mirandou, M. Fontana, and B. Arcondo, J. Mater. Process. Tech. **143–144** (2003) 420.
10. M. A. Ureña, A. A. Piarristeguy, M. Fontana, and B. Arcondo, Solid State Ionics **176** (2005) 505.
11. B. Arcondo, M. A. Ureña, A. Piarristeguy, A. Pradel, and M. Fontana, Physica B **389** (2007) 77.
12. A. Piarristeguy, J. M. Conde Garrido, M. A. Ureña, M. Fontana, and B. Arcondo, J. Non-Cryst. Solids **353** (2007) 3314.
13. M. A. Ureña, M. Fontana, A. Piarristeguy, and B. Arcondo, J. Alloy Compd. **495** (2010) 305.
14. B. Arcondo, M. A. Ureña, A. Piarristeguy, A. Pradel, and M. Fontana, Appl. Surf. Sci. **254** (2007) 321.
15. A. Piarristeguy, M. Ramonda, M. A. Ureña, A. Pradel, and M. Ribes, J. Non-Cryst. Solids **353** (2007) 1261.
16. A. Piarristeguy, M. Ramonda, N. Frolet, M. Ribes, and A. Pradel, Solid State Ionics **181** (2010) 1205.
17. A. A. Piarristeguy, M. Ramonda, and A. Pradel, J. Non-Cryst. Solids **356** (2010) 2402.
18. A. Fischer-Colbrie, A. Bienenstock, P. H. Fuoss, and M. A. Marcus, Phys. Rev. B **38** (1988) 12388.
19. J. D. Westwood, P. Georgopoulos, and D. H. Whitmore, J. Non-Cryst. Solids **107** (1988) 88.
20. J. D. Westwood and P. Georgopoulos, J. Non-Cryst. Solids **108** (1989) 169.
21. R. J. Dejus, S. Susman, K. J. Volin, D. L. Price, and D. G. Montague, J. Non-Cryst. Solids **106** (1988) 34.
22. R. J. Dejus, S. Susman, K. J. Volin, D. G. Montague, and D. L. Price, J. Non-Cryst. Solids **143** (1992) 162.

23. H. Iyetomi, P. Vashishta, and R. K. Kalia, J. Non-Cryst. Solids **262** (2000) 135.
24. L. Červinka, J. Bergerová, L. Tichý, and F. Rocca, Phys. Chem. Glasses **46** (2005) 444.
25. D. N. Tafen, D. A. Drabold, and M. Mitkova, Phys. Rev. B **72** (2005) 054206.
26. G. J. Cuello, A. A. Piarristeguy, A. Fernández-Martínez, M. Fontana, and A. Pradel, J. Non-Cryst. Solids **353** (2007) 729.
27. D. A. Drabold, Eur. Phys. J. B **68** (2009) 1.
28. L. S. R. Kumara, K. Ohara, Y. Kawakita, P. Jóvári, M. Hidaka, N. E. Sung, B. Beuneu, and S. Takeda, EPJ Web Conf. **15** (2011) 02007.
29. A. A. Piarristeguy, G. J. Cuello, A. Fernández-Martínez, V. Cristiglio, M. Johnson, M. Ribes, and A. Pradel, Phys. Status Solidi B **249** (2012) 2028.
30. J. R. Stellhorn, S. Hosokawa, Y. Kawakita, D. Gies, W.-C. Pilgrim, K. Hayashi, K. Ohoyama, N. Blanc, and N. Boudet, J. Non-Cryst. Solids **431** (2016) 68.
31. M. Mitkova and M. N. Kozicki, J. Non-Cryst. Solids **299–302** (2002) 1023.
32. M. N. Kozicki, M. Mitkova, M. Park, M. Balakrishnan, and C. Gopalan, Superlattice. Microst. **34** (2003) 459.
33. M. N. Kozicki, M. Park, and M. Mitkova, IEEE T. Nanotechnol. **4** (2005) 331.
34. R. S. Sharma, S. Singh, D. Kumar, and A. Kumar, Physica B **369** (2005) 227.
35. R. S. Sharma, D. Kumar, and A. Kumar, Turk. J. Phys. **30** (2006) 47.
36. R. S. Sharma, N. Mehta, and A. Kumar, Chin. Phys. Lett. **25** (2008) 4079.
37. I. T. Penfold and P. S. Salmon, J. Non-Cryst. Solids **114** (1989) 82.
38. I. T. Penfold and P. S. Salmon, Phys. Rev. Lett. **64** (1990) 2164.
39. A. Zeidler et al., in preparation.
40. H. E. Fischer, A. C. Barnes, and P. S. Salmon, Rep. Prog. Phys. **69** (2006) 233.
41. T. E. Faber and J. M. Ziman, Philos. Mag. **11** (1965) 153.
42. H. E. Fischer, G. J. Cuello, P. Palleau, D. Feltin, A. C. Barnes, Y. S. Badyal, and J. M. Simonson, Appl. Phys. A **74** (2002) S160.
43. P. S. Salmon, S. Xin, and H. E. Fischer, Phys. Rev. B **58** (1998) 6115.
44. V. F. Sears, Neutron News **3** (1992) 26.
45. P. S. Salmon, J. Non-Cryst. Solids **353** (2007) 2959.
46. R. A. Martin, P. S. Salmon, H. E. Fischer, and G. J. Cuello, J. Phys.-Condens. Mat. **15** (2003) 8235.
47. R. J. Dejus, D. J. LePoire, S. Susman, K. J. Volin, and D. L. Price, Phys. Rev. B **44** (1991) 11705.
48. C. J. Benmore and P. S. Salmon, J. Non-Cryst. Solids **156–158** (1993) 720.
49. D. Carré, R. Ollitrault-Fichet, and J. Flahaut, Acta Cryst. B **36** (1980) 245.
50. A. C. Barnes, S. B. Lague, P. S. Salmon, and H. E. Fischer, J. Phys.-Condens. Mat. **9** (1997) 6159.
51. Y. Wang, M. Mitkova, D. G. Georgiev, S. Mamedov, and P. Boolchand, J. Phys.-Condens. Mat. **15** (2003) S1573.
52. M. Mitkova, Y. Wang, and P. Boolchand, Phys. Rev. Lett. **83** (1999) 3848.
53. P. Pattanayak and S. Asokan, J. Appl. Phys. **97** (2005) 013515.
54. M. A. Ureña, M. Fontana, B. Arcondo, and M. T. Clavaguera-Mora, J. Non-Cryst. Solids **320** (2003) 151.
55. P. Kumar, S. N. Yannopoulos, T. S. Sathiaraj, and R. Thangaraj, Mater. Chem. Phys. **135** (2012) 68.
56. A. B. Bhatia and D. E. Thornton, Phys. Rev. B **2** (1970) 3004.
57. P. S. Salmon, P. R. Soc. Lond. A **437** (1992) 591.
58. M. Kastner, Philos. Mag. B **37** (1978) 127.
59. J. K. Burdett and O. Eisenstein, Inorg. Chem. **31** (1992) 1758.